Application of non-invasive geophysical methods (GPR and ERT) to locate the ancient foundations of the first cathedral of Puebla, Mexico. A case study

J Ortega-Ramírez, Maksim Bano, M T Cordero-Arce, L A Villa-Alvarado, C Chavez Fraga

Application of non-invasive geophysical methods (GPR and ERT) to locate the ancient foundations of the first cathedral of Puebla, Mexico. A case study

J.Ortega-Ramírez[1], M.Bano[2], M. T. Cordero-Arce[3], L.A.Villa-Alvarado[1]and C. Chavez Fraga[4]

Abstract

This article presents the results of a ground penetrating radar (GPR) and Electrical Resistivity Tomography (ERT) investigation carried out in the atrium of the Cathedral of Puebla to shed new light on the location of the original temple known as the "Old Cathedral". Historians who endeavor to reconstruct the past of this historical monument propose two hypotheses. To verify whether the foundations are located on the north-west or north-east side of the current cathedral, a GPR study was conducted with 200 and 400 MHz antennas. The study was completed with an ERT survey. The remains of the old cathedral were located and identified in the northwestern part of the atrium. Further anomalies related to subsurface structures and consistent with the ephemeral existence of a smaller temple, the "Sagrario", were detected. The GPR proved to be the most suitable method to investigate without causing damage suspected subsurface remains, thus protecting cultural heritage.

Keywords: Cathedral Basilica of Puebla, historical monuments, GPR, ERT

[1]INAH,Lab.deGeofísica,MonedaNo.16,CentroHistórico, CDMX,06060; jorteg@gmail.com

[2]Strasbourg University, EOST/UMR-7516, 5 rue René Descartes, Strasbourg, France; maksim.bano@unistra.fr

[3]Conservación de los Bienes Culturales de la Arquidiócesis de Puebla; mathe_co@yahoo.com.mx

[4]Escuela Taller de Capacitación en Restauración de Puebla, Av. 4 Ote. 211, Centro, 72000 Puebla, México; arq.cristofraga@gmail.com

Introduction

Monumental cultural heritage in all its physical forms is an important component of collective identity; it is a non-renewable resource that is being lost in an alarming way, not only due to the passage of time but also as a result of human intervention and natural hazards such as earthquakes, river overflow and landslides. A holistic approach, based on innovative study techniques and materials, is therefore needed for the protection and proper management of heritage buildings to improve the efficiency of rehabilitation and conservation actions.

In fact, the need to preserve the integrity of historical constructions led researchers to develop a variety of non-destructive geophysical techniques which have been successfully applied in several case studies to obtain information on the composition of structural elements or textural properties of the old masonry (Pérez-Gracia, *et al.*, 2000; Pieraccini et al., 2005; Yalciner, et al., **2009;** Solla *et al*., 2011; Arka *et al*., 2019; Deidana, 2019 and Ortega-Ramirez *et al*., 2019).

The Ground Penetrating Radar (GPR), for instance, has proven to be an efficient method to determine the thickness of buried structures, whether natural or anthropic, such as crypts or tombs, or to detect boundaries between different building materials (Goodman, D., 1994; Carcione, J.M., 1996; Jol, 2009; Johnston *et al*., 2018;Yalçıner, 2019). Electrical resistivity tomography (ERT) has also been successfully tested in archaeological surveys due to its high sensitivity (Gündgdu, et al., 2017; Jodry *et al.* 2019).

In this study, we use the GPR and ERT methods that can contribute in archaeological research not only to identify buried remains (which would otherwise require invasive studies) but also map large areas and have a broader view of anthropic activity in the subsoil to understand settlement dynamics. The great potential of these methods is their non-invasive nature during the data acquisition phase.

The Cathedral of Puebla is the second-largest in the country after Mexico City Cathedral. It is a complex and rich building, which is considered World heritage and stands out as a remarkable example of architectural, cultural and artistic legacy. The Cathedral of Puebla is an emblematic monument of the city, the history of which is closely related to that of the town founded *ex nihilo* in 1531. The different stages of its construction testify to the combined efforts of the Spaniards and the Indians to erect a monument that could service the growing population of Puebla before being converted into the bishop's see. The history of the cathedral could not be understood without the existence of an earlier temple, the "Old Cathedral", which was begun in 1536 and finished in 1539, but due to poor technological construction techniques and materials, rapidly presented serious problems and required constant reparations. It was finally declared unworthy of extensive reparations and demolished in 1649, and the construction of a new cathedral was decided and begun in 1575. There have been numerous attempts at reconstructing the history of this first temple and controversial theories put forth as to its location. In order to shed new light on these controversies, the Ministry of Culture and the diocese of the state of Puebla required us to survey the site with non-invasive techniques.

We prospected with GPR and ERT the surface of the atrium of the Cathedral of Puebla in Mexico. The objective was to test if there are actually remains of the first construction of the cathedral to validate one of the following hypotheses: i) the foundations are located on the northwest side of the current cathedral, or ii) they are located on the north side of the cathedral.

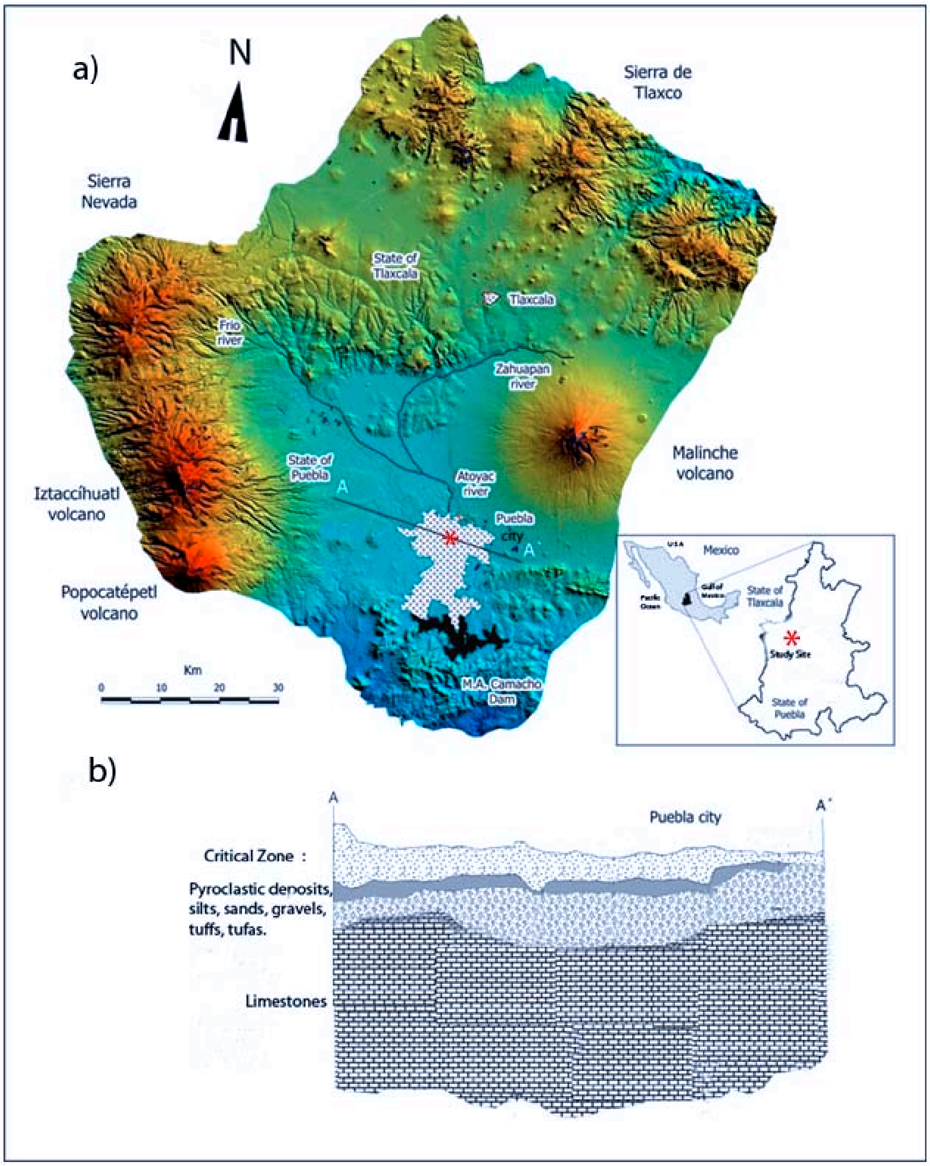

Fig. 1. a) Location of study area, asterisk indicates the city of Puebla. b) Geological section (A-A') showing different lithological formations (modified from Garfias *et al.*, 2010).

Site description

The Cathedral of Puebla is located in the state of Puebla in central Mexico at the latitude of 19.042705° N and longitude 98.198456°W, it is at2,182 m a.s.l., about 120 km southeast of Mexico City. The climate is mild and the precipitation is moderate during the summer. The annual mean temperature is 16.6° with a maximum of 21.3° in May and a minimum of 10.8° in February. The annual mean precipitation ranges from 650 to 900mm, with a maximum of 1000 mm. The study site is located in the central part of the Trans Mexican Volcanic Belt, a chain of mountains which spans across Central Mexico from the Pacific Ocean to the Gulf of Mexico and dates from Oligocene to Holocene or Recent. It is surrounded by three main volcanoes: Popocatépetl, Iztaccíhuatls and Malinche, the former active since 1994 (Fig. 1a).

The subsoil of the city of Puebla consists of carbonate rocks (limestone) formed during the Cretaceous and Tertiary periods covered by volcanic-clastic sediments and volcanic rocks interstratified with fluvial and lake deposits. In some places, there are deposits of tuffa produced by springs and interspersed with silt and clays as well as with aeolian sediments of volcanic origin. These sediments and rocks come from the surrounding volcanoes that produce lava flows, pyroclastic deposits and tuffs (cf. Fig. 1b). The city is located in an area with seismic activity due to its proximity to the Popocatépetl volcano.

Acquisition and processing of GPR and ERT data

The GPR is a geophysical method based on propagation/reflection of high frequencies (between 10 and 2600 MHz) electromagnetic (EM) waves. It is sensitive to the changes of EM properties of materials through which the waves are travelling. This method has multiple applications in different areas such as geology, environmental pollution, civil engineering (bridges, walls, buried pipes, airports, etc.) and glaciology as well as in cultural heritage (archeology, painting on wood, historical monuments, etc.). The GPR system is generally composed of a central unit, a transmitting and receiving antenna, and a computer. The central unit produces short electromagnetic pulses (from 1 to 60 ns) that are radiated to the ground through the transmitting antenna. When electromagnetic waves or pulses find a buried discontinuity (objects/cavities or an interface between two geological layers), the waves are diffracted/reflected and a part of the energy returns to the surface and is recorded by the receiving antenna. The other part of EM energy propagates into the soil through the discontinuities. The speed of the GPR waves in the medium depends on the water content (humidity) of the soil, the higher the humidity in the soil, the lower the velocity of GPR waves. For the GPR study conducted on the surfaces of the cathedral atrium, we calculated an average wave speed of 0.065 m ns (dielectric constant of 21), which indicates a soil with high humidity. The higher the frequency of the antenna used, the higher the vertical resolution and the lower the investigation depth.

Fig. 2. GPR measurements in the atrium of Puebla Cathedral:a) With a 400 MHz frequency antenna. b) With a 200 MHz frequency antenna.

We used the GPR system of SIR-3000 with monostatic shielded antennas of 200 and 400 MHz (**seeFig. 2**).The GPR measurements were conducted on 7 surfaces of different sizes within the atrium. For 3D acquisition we carried out parallel lines along a single direction with spacing of 0.50 m for the 200 MHz antenna and 0.25 m for the 400 MHz antenna. The trace interval was 0.01 m for both antennas. The first 3 surfaces (named S1, S2 and S3) were along the atrium on the west side (S1), in front of the main entrance of the Cathedral (S2) and on the south-west side opposite the ossuary (S3), respectively (see Fig. 3). The surfaces of the northern atrium were fragmented into 4 small surfaces (S4, S5, S6 and S7 respectively) due to the installation of luminaries (Figs. 3 and 4).Table 1 shows the profile spacing (Δy), sampling interval (dx), the frequency used and the size of each surface area (S1, S2,…, S7).

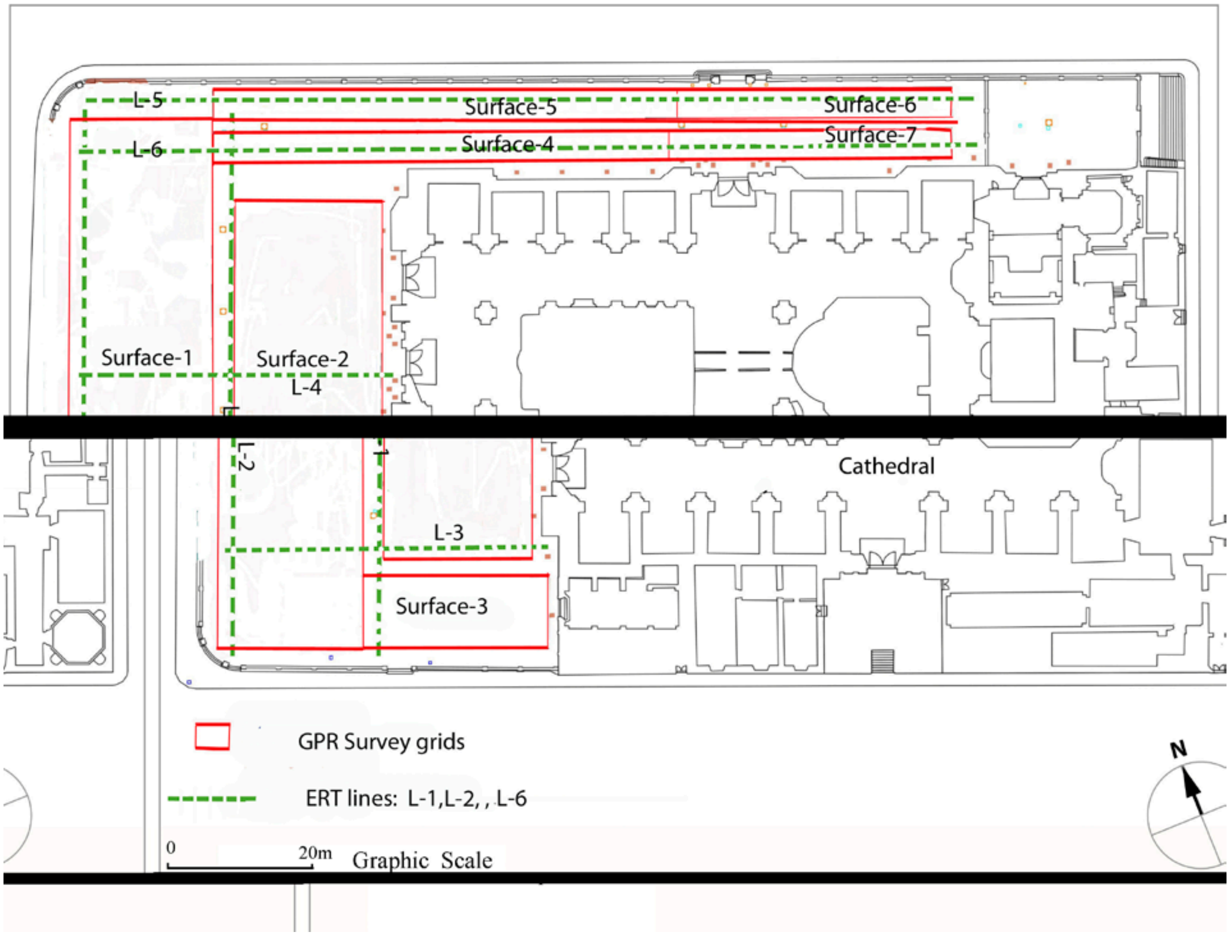

Fig. 3. Survey study area showing the GPR surfaces in red (S1, S2,..., S7) and ERT lines in green (L-1, L-2,…, L-6).

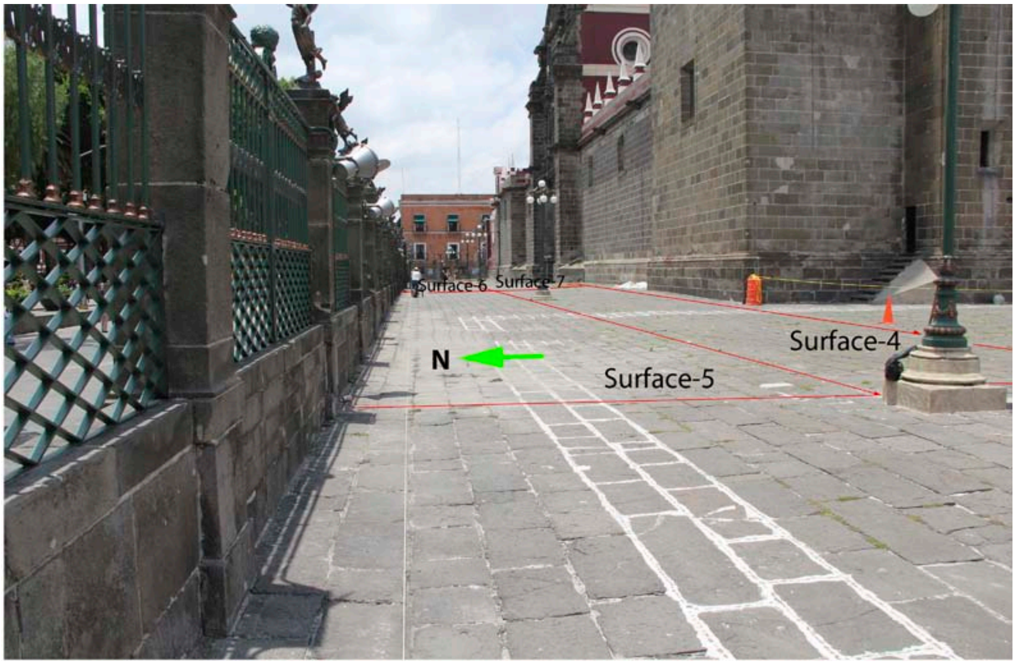

Fig. 4. North side of the cathedral, note the distribution of the four surfaces prospected with a 400 MHz GPR antenna (S4, S5, S6 and S7 areas).

Table 1 Profile spacing (Δy), sampling interval (dx) and surface areas (S1, S2,…, S7).

Antenna (MHz)	Δy (cm)	dx (cm)	Area-S1 (m x m)	Area-S2 (m x m)	Area-S3 (m x m)	Area-S4 (m x m)	Area-S5 (m x m)	Area-S6 (m x m)	Area-S7 (m x m)
400	25	1	20 x 74	21.5 x 49		4.5 x 68	4.25 x 68	4.25 x 40.5	4.25 x 40.5
200	50	1	20 x 74		10.25 x 28				

For the processing of GPR data we used the software package of Radan 7 for Windows and Radlab (written in Matlab) developed at 'Institut de Physique du Globe' laboratory (Strasbourg, France). The processing sequence involved time-zero shift, low-frequency removal or DC filtering (dewow), amplitude gain (linear and/or exponential), and finally, band-pass filtering (100-400 MHz and 200-800 MHz for 200 and 400 MHz antenna, respectively).The velocity of the electromagnetic (EM) waves was estimated by using different diffraction hyperbolas observed in the 2-D GPR profiles. We determined an average wave velocity of 0.065 m /ns, which indicates a soil with high humidity. For the 3-dimensional (3D) presentation of GPR data we used Radan and ReflexW software. The time window, the value of the velocity, and the vertical resolution are given in Table 2 for each antenna.

Table 2Time window, frequency, velocity and vertical resolution (λ/4 criterion).

Architectural element	Time Window (ns)	Antenna (MHz)	Velocity (m/ns)	Resolution(cm)
Atrium	62	400	0.065	4
Atrium	98	200	0.065	8

The ERT method consists in injecting an electrical current to the subsoil by means of two electrodes and measuring the voltage (or potential difference) between two other electrodes. The principle of measurements is based on the hypothesis of a stationary electric current in a homogeneous and isotropic conductive medium (Ohm's law). The conductivity (resistivity) of the soil depends drastically on the presence of fluids in the soil; the higher the humidity in the soil, the higher the conductivity (the lower the resistivity). Changes of the conductivity (resistivity) can be measured by the ERT method. Since 1950s, the electrical resistivity method has proven efficient in prospecting buried masonry structures and archaeological remains (Hesse, *et al.*, 1986; Kampke, 1999; Tsokas et al., 2008; Di Maio *et al.*, 2012). It is an effective method to detect moisture caused by capillarity rise in historical monuments, thus avoiding degradation and disaggregation of the structure. We used the ERT system of OYO Corp. (McOHM-21, Model 2116) equipped with 32 flat electrodes spaced at 3.5 m. We performed six ERT lines named L-1, L-2,…, L-6 and shown in Fig. 3 by green doted lines. The ERT profiles were modeled and inversed by using the Res2Dinv and Geotomo Software.

GPR and ERT Results

Although all GPR and ERT profiles were processed and interpreted, for the current study we present only the most important results. The GPR profiles of S1 area are oriented from south to north and spaced every 20 cm. (Fig. 3). Each profile was processed to eliminate electronic and background noise and filters were applied. In Fig. 5 we show the processing of the first thirty meters of profile-1(on the left side of S1, see also Fig. 3) obtained with 200 and 400 MHz antennas, respectively. The investigation depth is about 1.60 m for both antennas. As the vertical resolution is better with a 400 MHz antenna, we decided to use it in most of the surveyed areas (See Table 1). Additionally, a 3D model was developed to determine the geometry of the specific features that could correspond to old buried archeological structures (see Fig. 6).

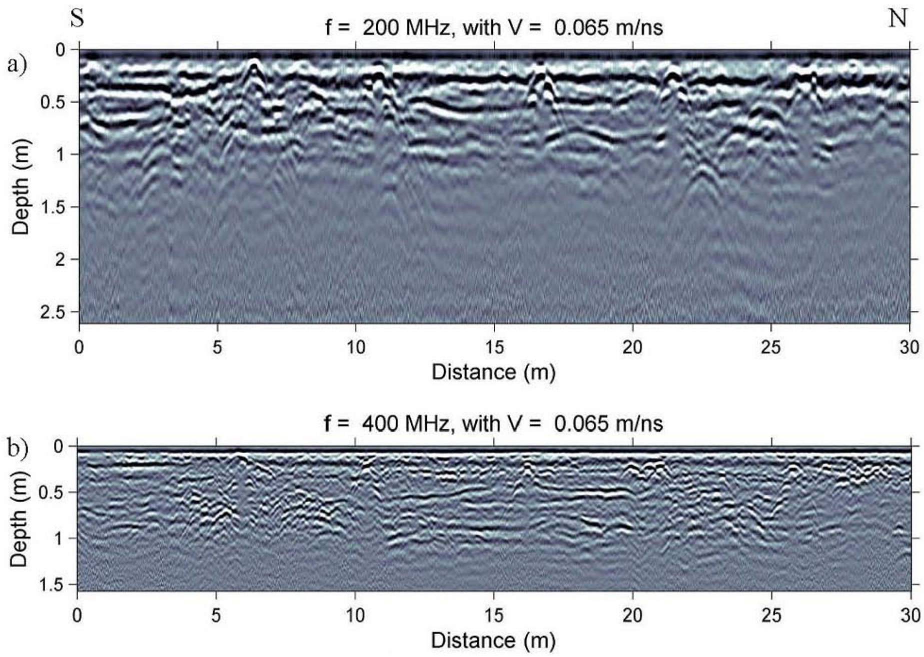

Fig. 5. Example of a 2D GPR profile measured on the Surface-1 with a) 200 and b) 400 MHz antennas, respectively. We only show the first thirty meters of profile1. Note the presence of multiple reflections/diffractions coming from archeological buried structures.

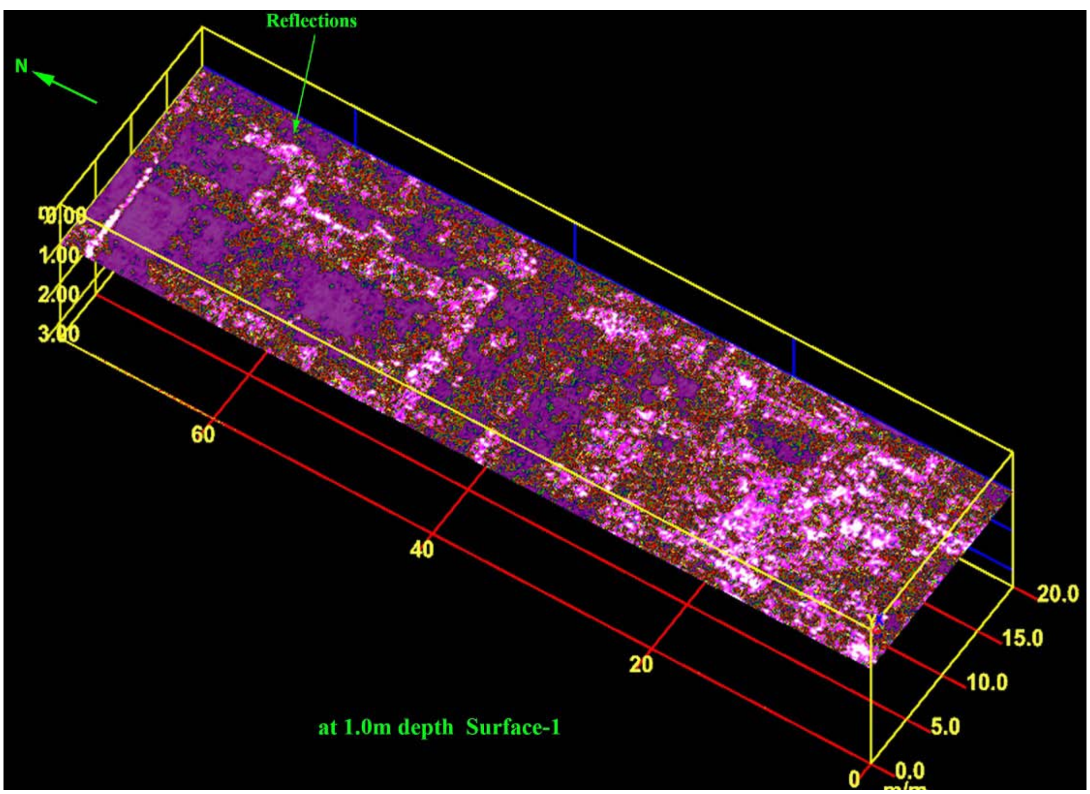

Fig. 6. 3D presentation of S1 area at a depth of 1 m (depth slice); the antenna used is of 400 MHz.

In Fig. 7a we present a depth slice at 1 m depth (S2 area) where we observe a highly reflective zone, the geometry of which could correspond to remnants of old foundations. The profiles are oriented from south to north and spaced every 25 cm. Figs. 7b and 7c show the ERT profiles L-4 and L-3, respectively. We used 16 flat electrodes spaced every 3.5 m. The high resistive anomalies indicated by white arrows correspond to the old foundations visible in the depth slice of Fig. 7a (see white arrows).

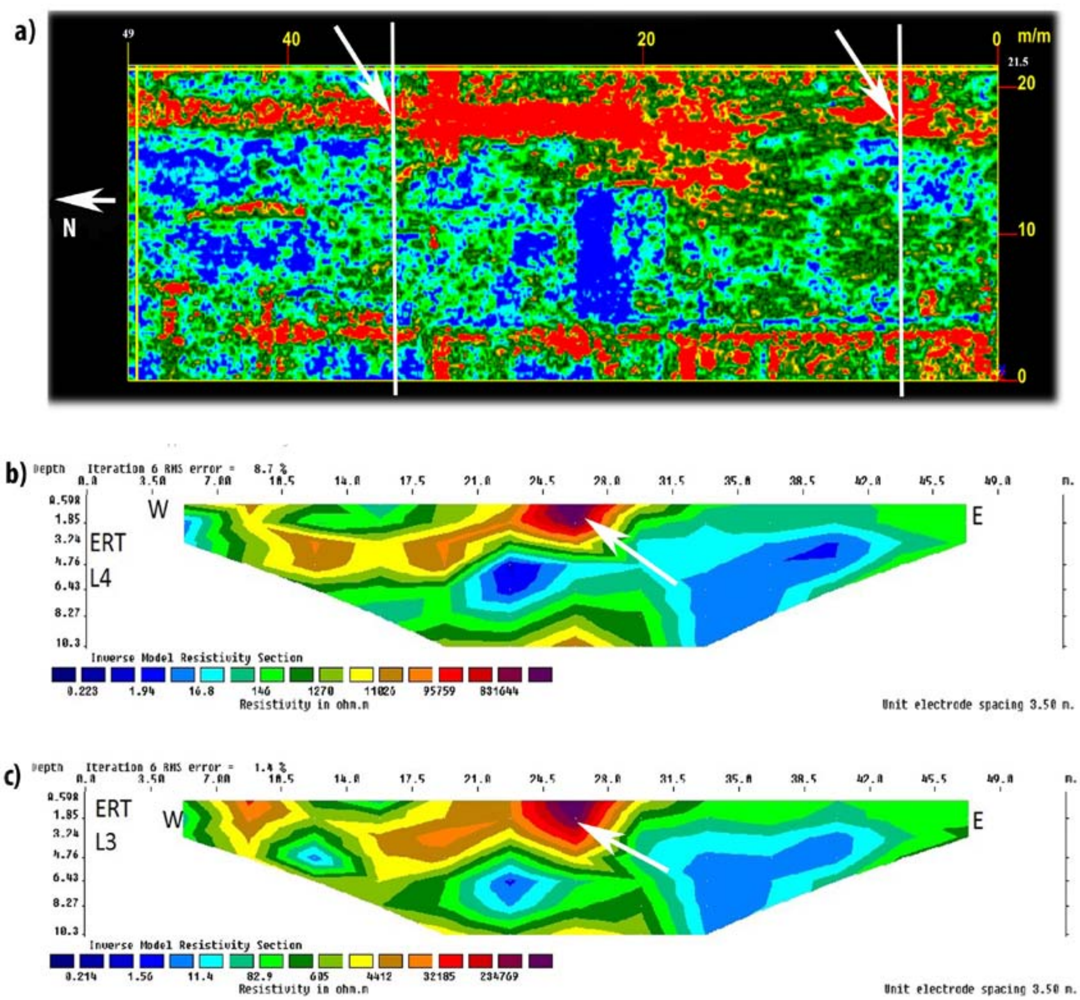

Fig. 7. a) The depth slice at 1 m depth with a 400 MHz antenna, S2 area. Note the distribution of the reflections (in red) coming probably from a well-defined geometric settlement. b) and c) show the ERT profiles L-4 (white line on the left) and L-3 (white line on the right), respectively. The white arrows indicate high resistive anomalies in accordance with high reflective zones (in red) shown by white arrows in the depth slice of a)

Figure 8 shows a picture of S3 area on the south side of the cathedral close to the ossuary, in front of “Aguadores”. From the depth slices at 25 cm depth (Fig. 8a) we observe the geometry of a 2.5 m wide structure (see white arrows) located in the northeastern part. This structure is present down to 50 cm depth (Fig. 8b) and could probably correspond to an ossuary, it disappears beyond this depth. On the 1.5 m depth slice (see Fig. 8c) we observe longitudinal shapes, the origin of which is unknown.

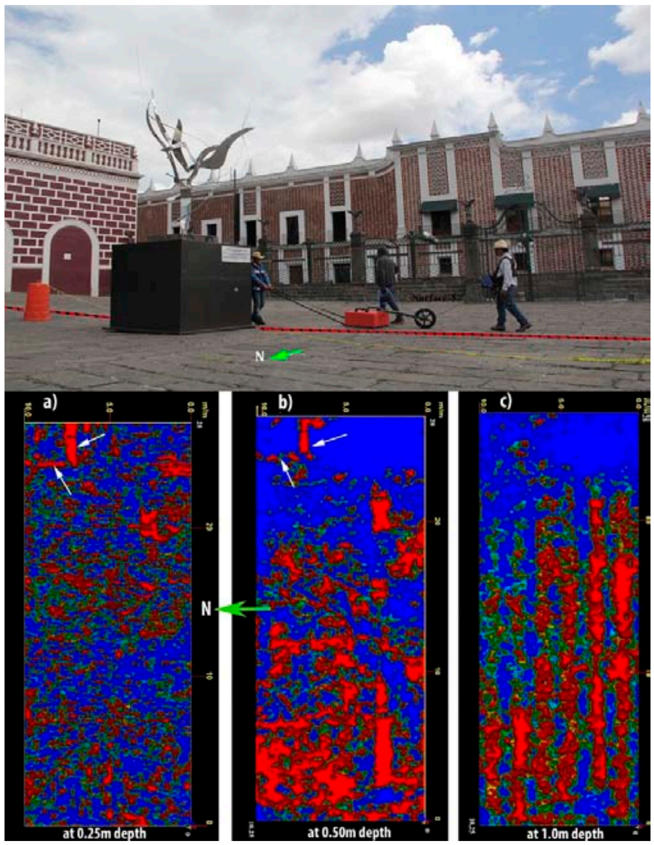

Fig. 8. Photo of S3 area in the front of “Aguadores” prospected with the 200 MHz antenna. a), b) and c) below show three depth slices at 25 cm, 50 cm and 1.5 m depth respectively. The structure indicated by the white arrows could probably correspond to an ossuary.

On the S4 area, located in the northern part of the cathedral (see also Fig. 4), the most outstanding results are observed at1 and 1.5 m depth. The red anomalies visible in Figs. 9a and 9b show high reflectivity zones and could correspond to the old foundations.

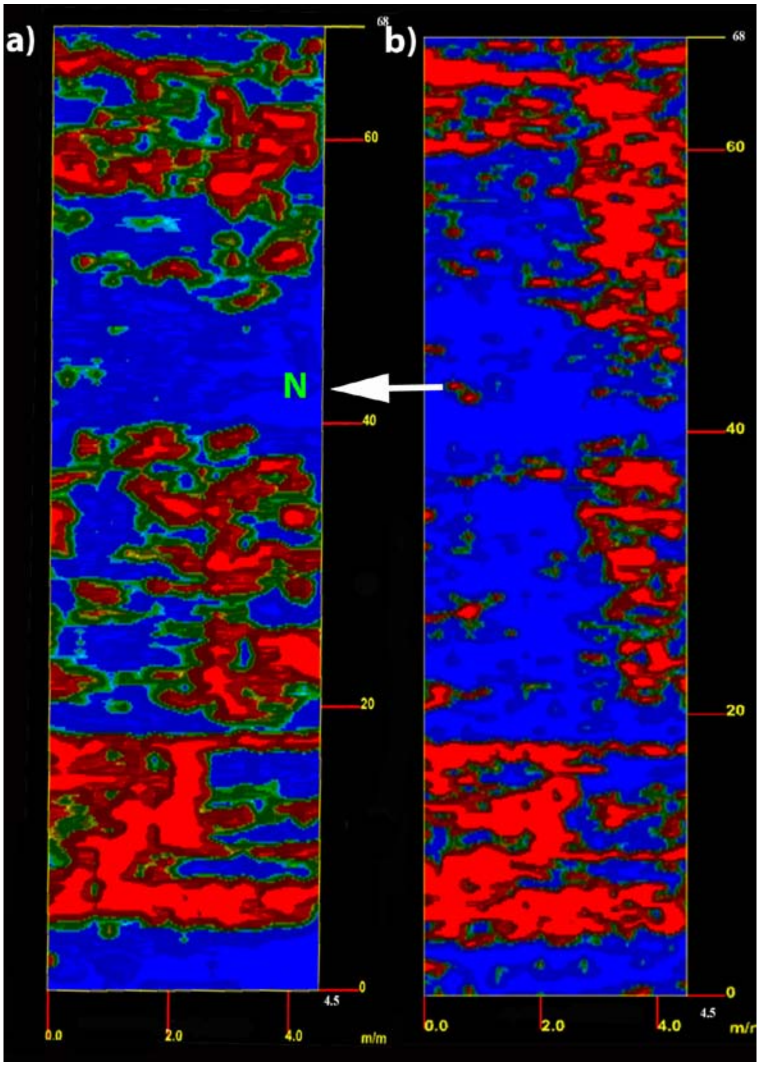

Fig. 9. S4 area in the northern part of the cathedral. Depth slices at 1m(a) and 1.5 m (b) depth, respectively. The red anomalies show zones with high reflectivity and could correspond to old foundations.

The S5 area is located almost symmetrically north of the S4 area, and only separated from it by a line of luminaries oriented from east to west (see also Fig. 4). The most outstanding features are observed at 1 and 1.5 m depth where two highly reflective zones appear on both sides to the east and west (see Fig. 10). As in the previous surface, they probably correspond to old foundations.

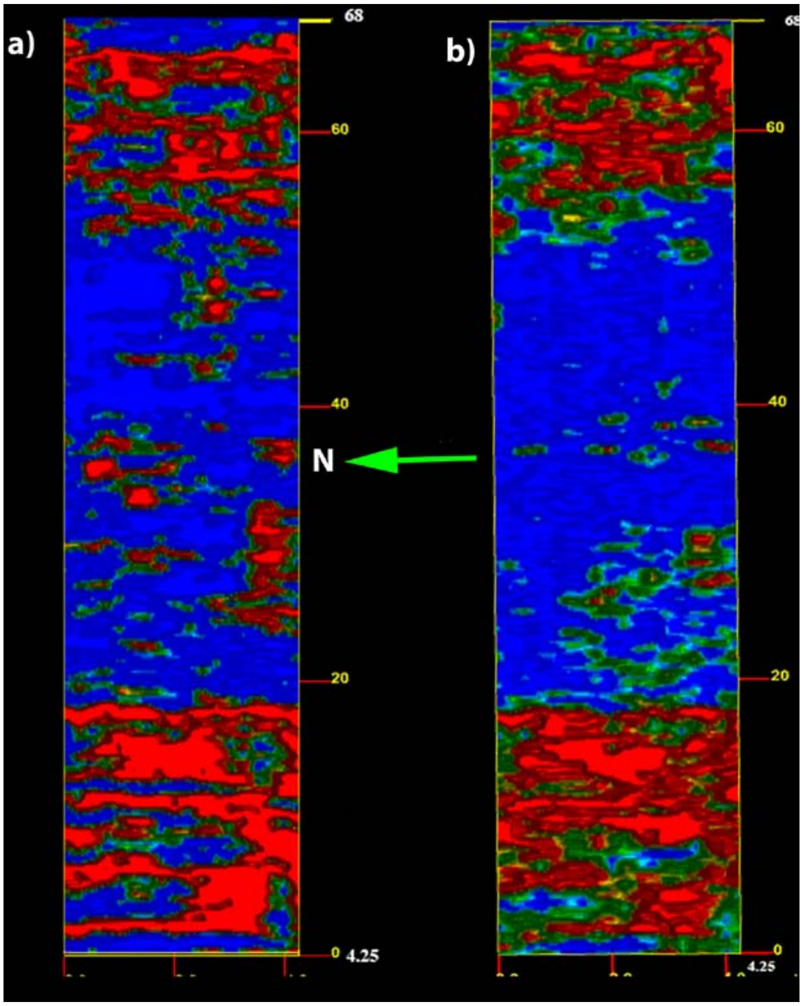

Fig. 10. Depth slices at 1 m (a) and 1.5 m (b) depth in the S5 area. The red anomalies indicate highly reflective zones and probably correspond to old foundations.

In the S6 area, located to the north and bordering the fence of the cathedral (see Fig. 4), the most outstanding features are identified at a depth of nearly 1.0 m where red anomalies which are perpendicular to the fence, can be observed. At 1.5 m depth, these features are even accentuated, and could correspond to remains of a buried construction structure (see Fig. 11).

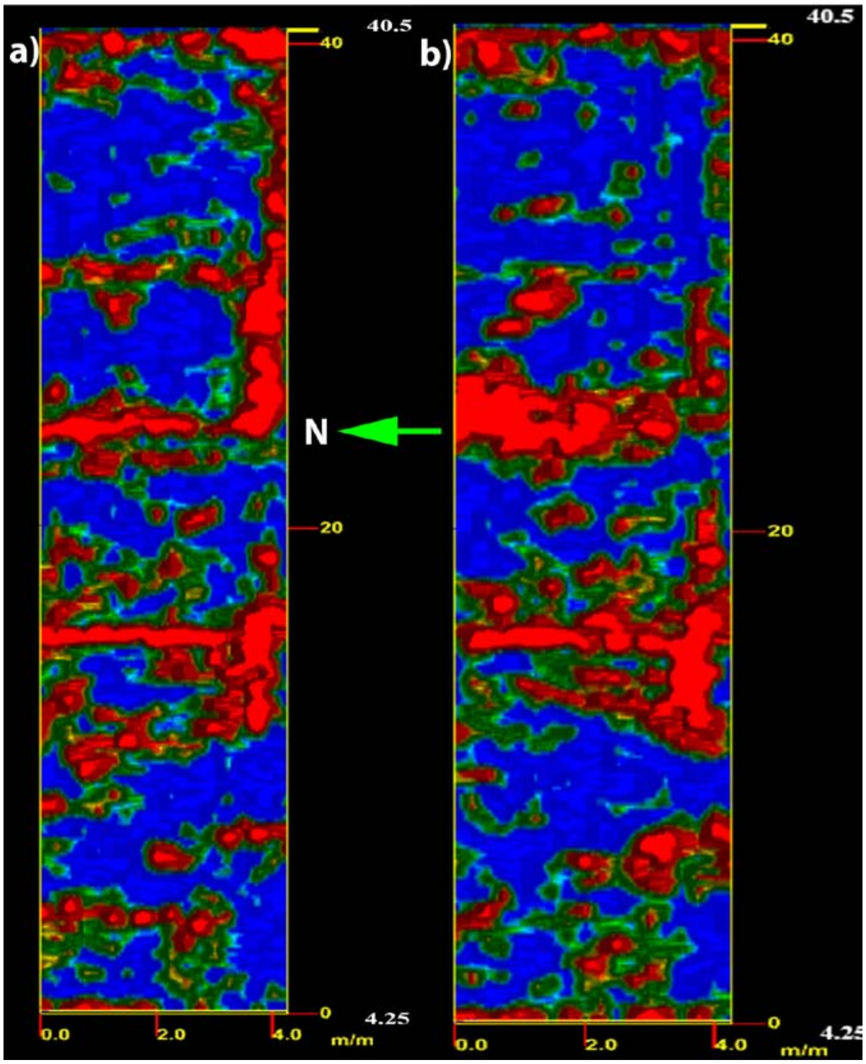

Fig. 11. Depth slices at 1 m (a) and 1.5 m (b) depth in the S6 area. The red anomalies show high reflectivity zones, probably corresponding to remains of buried construction structures.

The S7 areais located south of the S6 area and separated from it to the north by a series of luminaries (see Fig. 4). On this surface, the identified features are geometrically less precise than on the previous surfaces (Ortega and Villa Alvarado, 2018).

Discussion of Results

Among all the surveyed surfaces the S1 area of 20m x 74m in the western atrium presents reflections that define a more elaborate geometry than the other ones. In Fig. 12 we show a 3D presentation of the depth slice at 1 m depth in which shapes that evoke diverse architectural structures of varying dimensions can be observed. Due to their configuration, they can be interpreted as the masonry foundations of the first cathedral (ancient temple), in accordance with hypothesis 1according to which the old foundations are located on the northwestern side of the current cathedral. The unit measure used at that time was the "vara" equivalent to 0.8359 m in the decimal metric system, subdivided into 4 parts and each of them in twelve fingers and each finger in four grains (Rocha-Martinez, 2011).In the central part of the temple, several elements distributed geometrically appear at regular distances. For example, from the right side wall to the element that seems to be the base of a column, there is a distance of 5.5 varas (4.59745m). In the central nave, the distance between columns in the longitudinal direction is 5 varas (4.1795m) and transversally it is 9 ½ varas and 1 sesma (8.0796 m; 1 sesma = 0.1393m).

According to Chavez-Fraga (2018), who compared the measures of the first cathedral of Puebla built in the first half of the 16th century with the architecture of similar contemporaneous temples in New Spain, constructed with masonry and/or adobe walls and wooden deck on pillars without arches, the results of the S1 area correspond to the remains of old foundations that are 70 "varas" (58.5134 m) long from the main altar to the entrance of the church and 23 "varas" (19.2258 m) wide. The wall thickness was estimated to be 1.2539 m (1.5 varas), while the thickness of the foundations was estimated at two "varas" or 1.6718 m (Fig. 13). The surveyed area in Fig. 13 does not include the whole west side of the remains because of the existence of the current perimeter wall. To infer the lacking distance (of the) in width (19.2258 m in Fig. 13) we added 4.5975 m (5.5 varas) on the left side of the central column to respect the symmetrical pattern of this type of constructions. The axis of symmetry passes through the middle of the distance (8.0796 m) between both rows of columns (see Fig. 14).

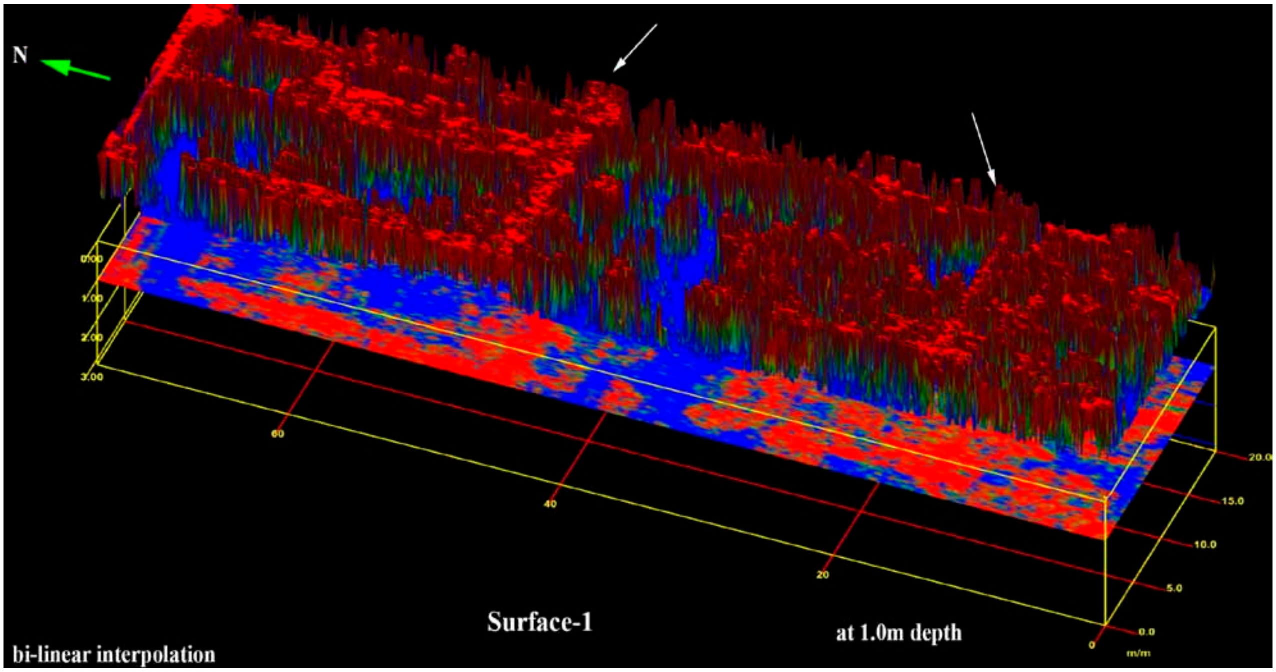

Fig. 12. Depth slice of S1 area at 1 m depth presented in 3D using cross and in-lines interpolation of the data (bilinear interpolation). The most reflective areas in red, indicated by white arrows, define buried geometric building structures.

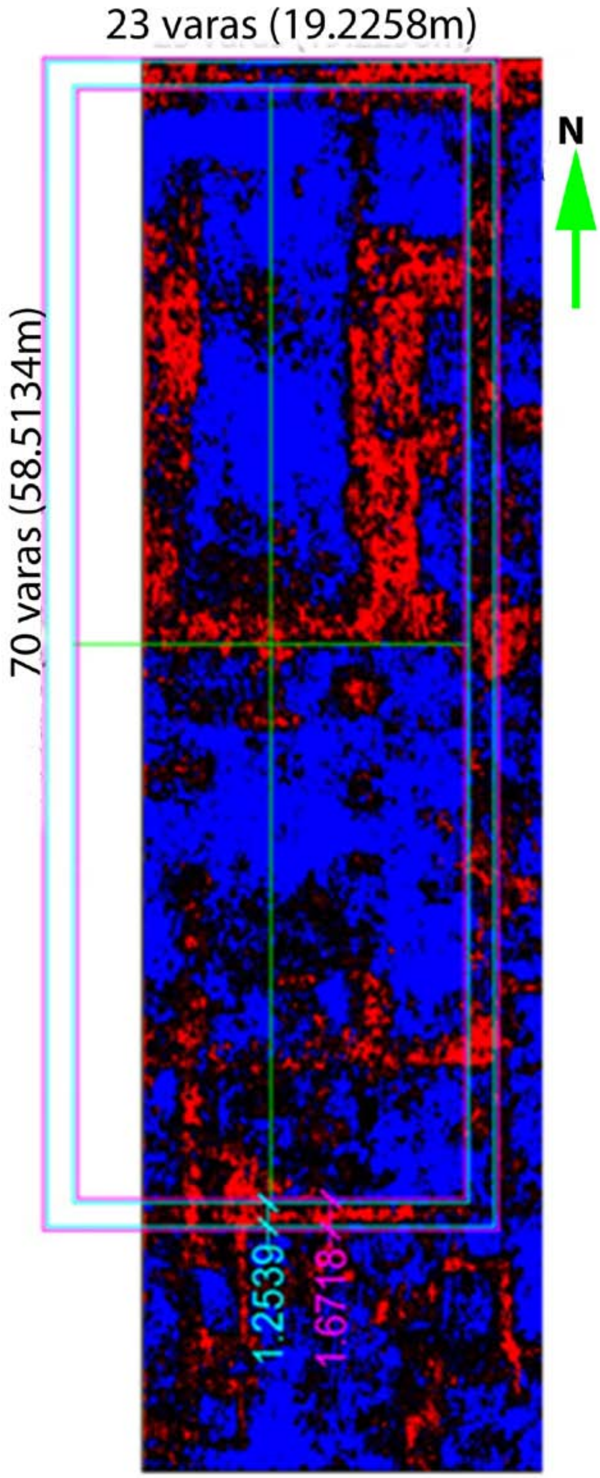

Fig. 13. Depth slice of S1 area at 1 m depth. Note the presence of ‘El Sagrario’ in the northern part (see the blue zone cross-shaped area).The light blue rectangle demarcates the area of the ancient temple where the thickness of the walls is estimated to be about 1.2539 m, and the magenta color refers to the foundations about 1.6718 m thick.

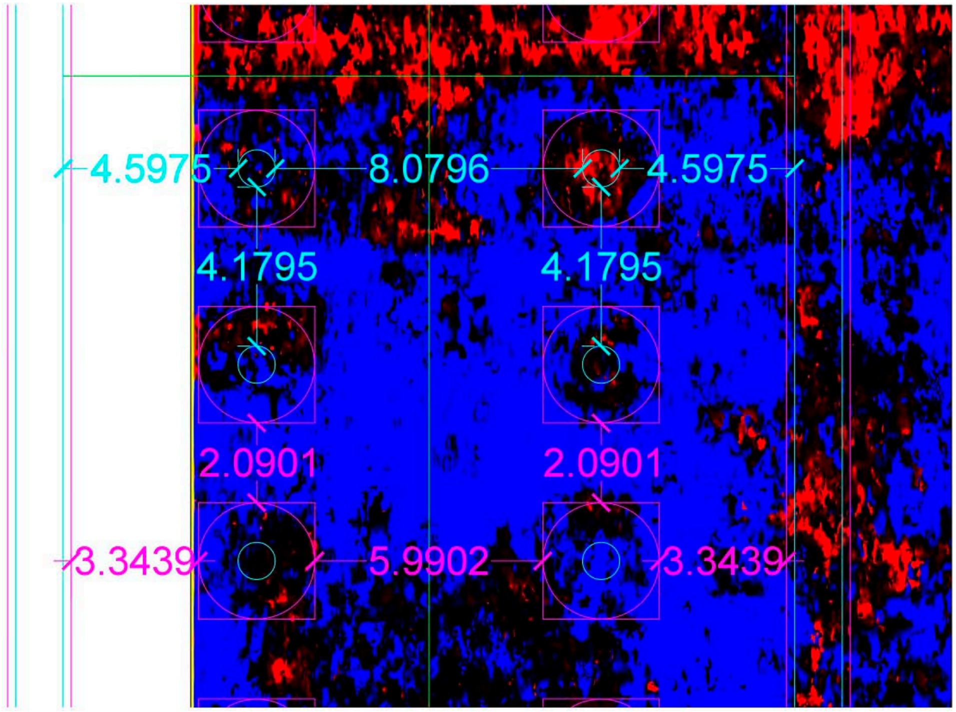

Fig. 14. The numbers show the distances from the columns to the walls, between the columns and between both rows of columns: a) in blue the centre to centre distance; b) in magenta from the bases of the columns.

According to the GPR amplitude map at 1m depth (Fig. 13), the remains of two rows of 6 columns each can be clearly distinguished in the southern part of the nave. In the northern part however, they are not clearly visible, probably because a subsequent structure, “El Sagrario” was built in that part and demolished later on (Molero Sañudo, A.P., 2014; Ríos Yanes M., 2018). Nevertheless, it is very likely that six more pairs of columns existed in this part as is hypothesized by Chavez-Fraga (2018) who considers that twelve columns would not have been sufficient to support the roof of the church (Figures 15 and 16). This hypothesis furthermore is consistent with the dimensions of the church as well as with the construction style at that time.

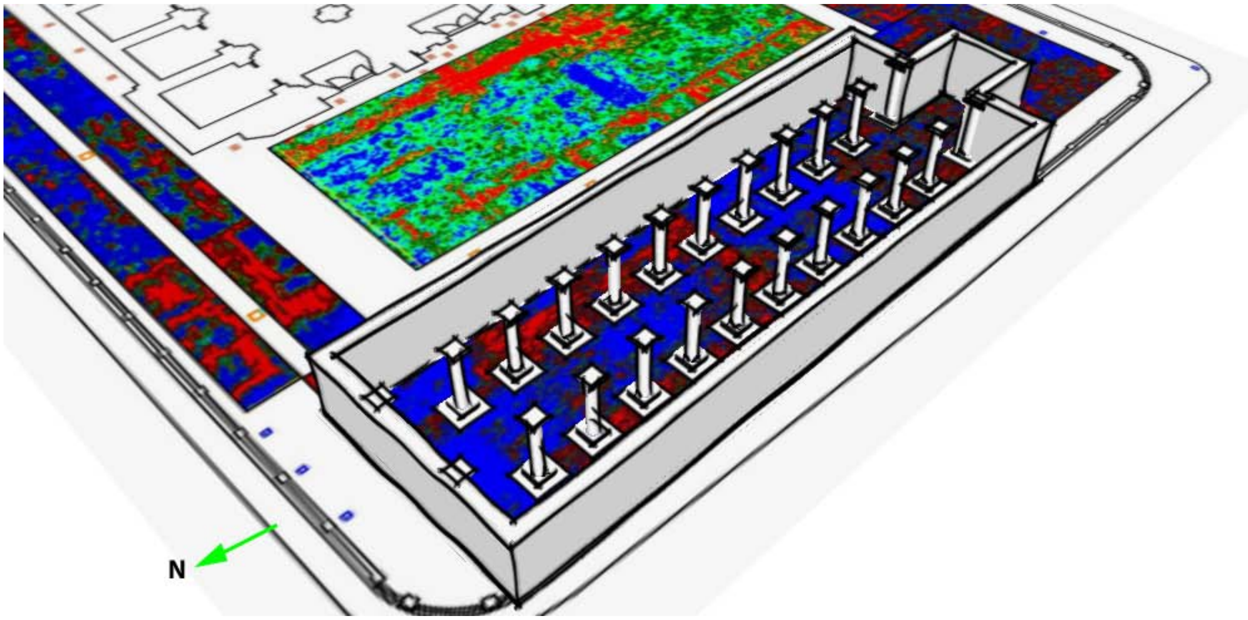

Fig. 15. Hypothetical reconstructions of the columns from the GPR depth slice in background. The red anomalies indicate the reflective zones corresponding to walls and construction structures.

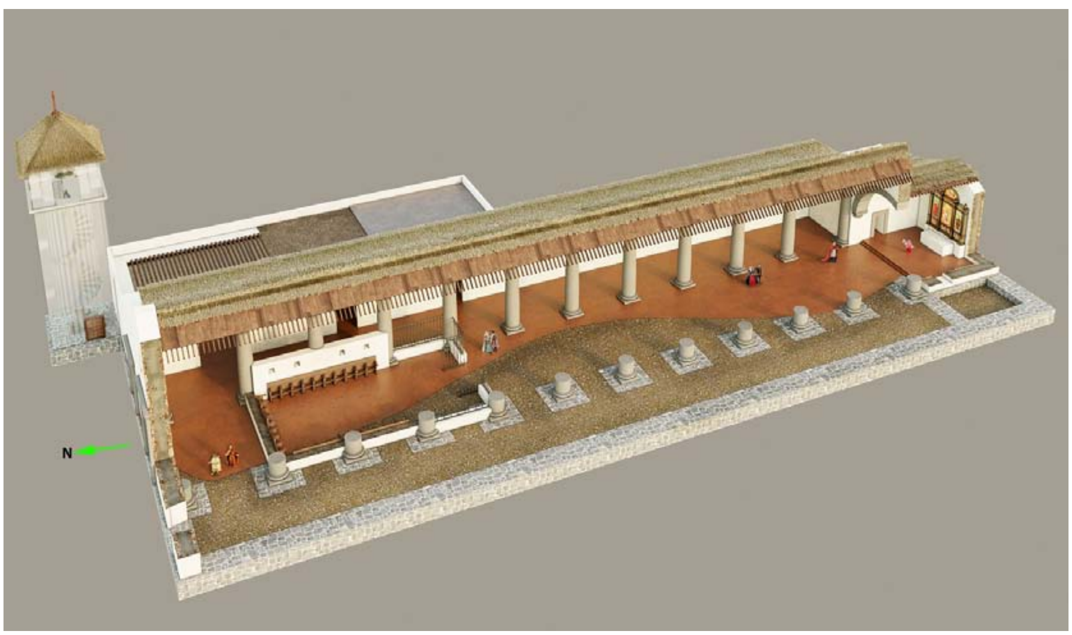

Fig. 16. Reconstruction of the temple considering twelve columns per side.

In the annexed spaces to the east of the temple, buried structures were also identified that could correspond to lateral chapels built with a regular pattern. Whereas in the annexed spaces to the north east of the temple(S4, S5, S6 and S7 areas) buried structures are built without a regular pattern, which suggests that they were built according to the needs or sponsorship obtained through time (see Fig. 17).

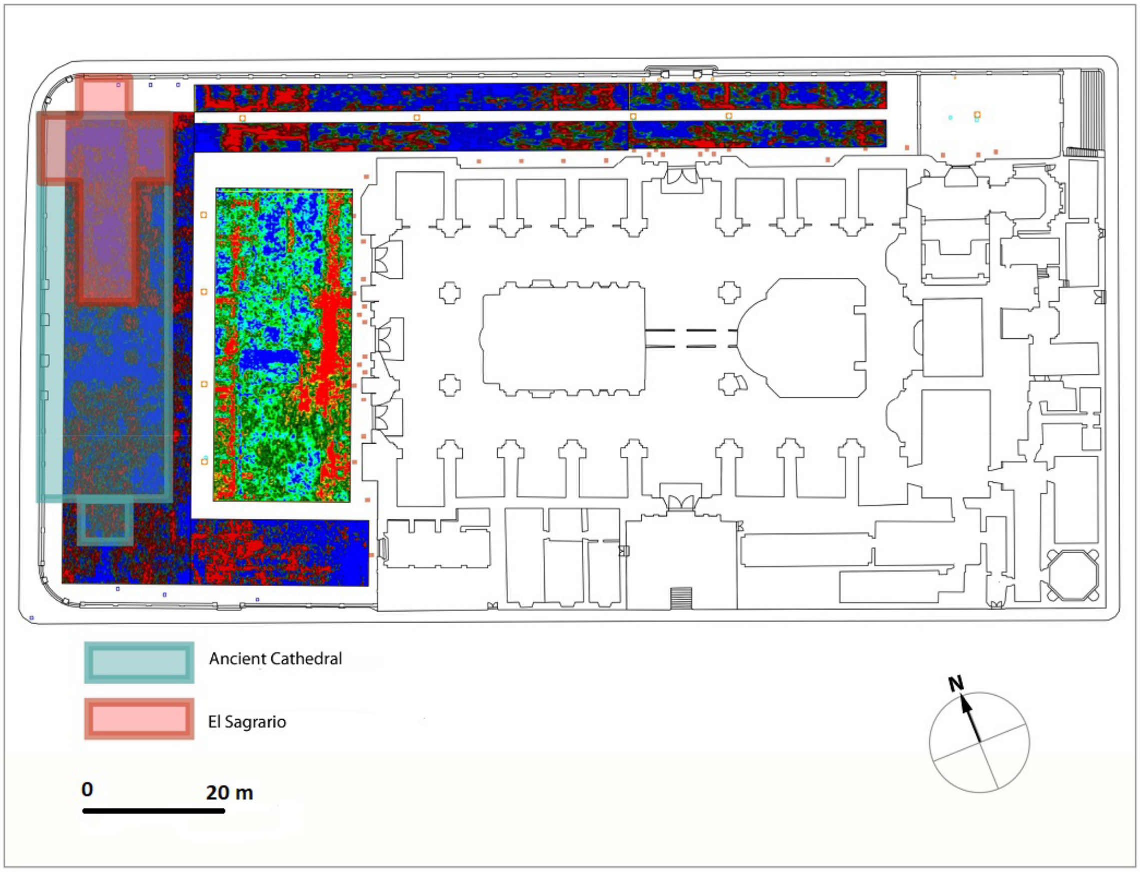

Figure 17 Architectural plans with the integration of all GPR results.

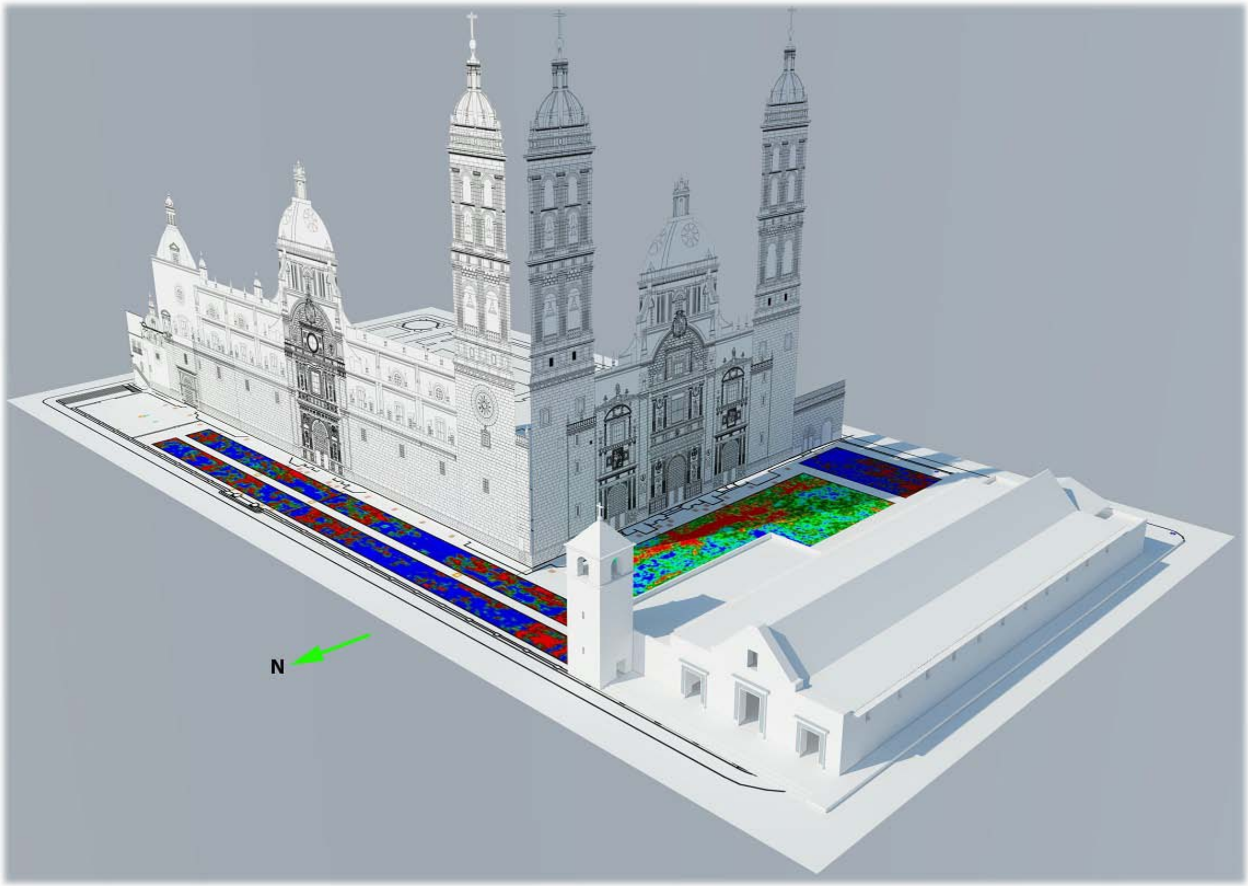

Fig. 18. 3D model integrating the ancient temple at the front with the current cathedral in the background and the depth slices of GPR images at 1 m depth showing the remains of building foundations interpreted as chapels.

Conclusion

The remains of the old cathedral were located and identified in the northwestern part of the atrium within the so-called Surface-1. The reflections at one meter of depth indicate the old foundations. The maximum depth penetration was about 1.60 m due to the high water content of the subsurface determinated by the high value of the dielectric constant (about 21). Looking at the depth slices of different grids, the best results were obtained with the 400MHz antenna using bilinear interpolation (by interpolating the cross and in-lines profiles) of the S1 area. Although the results do not appear with the same clarity on all the surveyed surfaces, by analyzing and combining them, it is possible to infer the extent of the architectural remains. Considering their shape in correlation with the unit of measures (varas) used at that time and the historical information, it may be concluded that the remains are part of the old cathedral and ‘El Sagrario’ temple reported in Chavez Fraga (2018).

It may be assumed that the features interpreted in the northern part at a depth of one meter as the remains of pillars aligned in two rows continue in the southern part of the surface although they are not clearly visible on the depth slice. This implies that there were probably two rows of twelve pillars, an assumption which is consistent with the size of the church nave.

The georadar proved to be very well adapted to identify subsurface structural remains on sites where it is impossible to apply invasive methods or techniques. The electrical resistivity tomography proved to be a complementary method to solve or reduce the uncertainties associated with indirect evaluations.

Acknowledgements

We thank the Rector of the Basilica Cathedral of Puebla, Rev. José Francisco Patricio Vázquez Ramírez and the staff of the restoration school, especially Mter. Laura Rosas Gutierrez, who helped us to accomplish the geophysical acquisition. The authors thank the ‘Centre National de la Recherche Scientifique’ (CNRS/UMR7516) and EOST/Strasbourg University for financially supporting José Ortega to visit several times the ‘Institut de Physique du Globe de Strasbourg’. We are also indebted to Danielle Duda who reviewed earlier drafts of this manuscript and contributed to its improvement.

References

Arka, I., Balkaya, Ç., Pülz, A., Alanyali, H.S., Kaya, M. A., 2019. Integrated geophysical investigations to reconstruct the archaeological features in the Episcopal district of Side (Antalya, Southern Turkey. *Journal of Applied Geophysics*, 163: 22-30.

Carcione, J. M., 1996. Ground radar simulation for archaeological applications. *GeophysicalProspecting*, **44**, 871-88.

Chavez-Fraga, C. M., 2018. La iglesia mayor de Puebla bajo la mirada del siglo XXI, Cap. VIII, pp. 201-241. "*La antigua Catedral de Puebla*". Secretaria de Cultura y Turismo del Edo. De Puebla.

Deidana, R. 2019. The contribution of geophysical prospecting to the multidisplinary study of the Sarno Baths, Pompeii. *Journal of Cultural Heritage*, https://doi.org/10.1016/j.culther.2019.04.018.

Di Maio, R.,Meola C., GrimaldiM. and Pappalardo U., 2012. New Insights for conservation of villa Imperiale (Pompei, Italy) through nondestructive exploration. *International Journal of Architectural Heritage*, **6**: 562–578,

Jodry, C., Palma Lopes, S., Fargier, Y, Sanchez, M. and Côte, Ph. 2019. 2D-ERT monitoring of soil moisture seasonal behavior in a river levee: A case study. *Journal of Applied Geophysics*, 167:140-151.

Johnston, B., Ruffell, A., McKinley, J., Warke, P., 2018. Detecting voids within a historical building façade: A comparative study of three high frequency GPR antenna. *Journal of Cultural Heritage*, **32**:117-123.

Jol, H.J. (Editor) 2009. Ground Penetrating Radar Theory and Applications.Elsevier.

Gárfias, J., Arroyo, N., Aravena, R. 2010. Hydrochemistry and origins of mineralized waters in the Puebla aquifer system, México. *Environ Earth Sci*, **59**:1789-1805.

Goodman, D. 1994. Ground-penetrating radar simulation in engineering and archaeology. *Geophysics*, **59**(2):224-32.

Gündgdu, Y., N., Casansayar, E., and Genc, E. 2017. Rescue Archaeology Application: Investigation of Kuriki Mound Archaeological Area (Batman, SE Turkey) by using Direct Current Resistivity and Magnetic Methods. *JEEG*, June 2017, V. **22** (2):177-189.

Hesse, A., Jolivet, A., and Tabbach, A. 1986. New prospects in shallow depth electrical surveying for archaeological, pedological applications. Geophysics 51, pp.:585-594.

Kampke, A., 1999. Focused imaging of electrical resistivity data in archaeological prospecting, J*ournal of Applied Geophysics*, **41**:215–227.

Molero Sañudo, A.P., 2014. La Catedral de Puebla: historia de su construcción hasta la remodelación neoclásica de José Manzo y Jaramillo. Ph.D., Universidad Complutense de Madrid.

Ortega-Ramírez, J., Bano M., Lelo de Larrea-López, L., Robles-Camacho, J., Ávila-Luna P. and Villa-Alvarado, L., 2019. GPR measurements to identify cracks and textural arrangementsin the altar wall of 16th century Santa Maria Huiramangaro Church, Michoacán, Mexico.*Near Surface Geophysical (NSG)* Journal,doi: 10.1002/nsg.12040.

Ortega-Ramirez, J., and Villa-Alvarado, L., 2018. Ventanas al ayer: Aplicación de métodos geofísicos no invasivos para localizar los vestigios de la Antigua Catedral. , Cap. VI, pp. 125-153. "*La antigua Catedral de Puebla*". Secretaria de Cultura y Turismo del Edo. De Puebla.

Pérez Gracia, V., Canas, J. A., Pujades, L. I.G., Clapés, J., and García, F. 2000. GPR survey to confirm the location of ancient structures under the Valencia Cathedral (Spain). J*ournal of Applied Geophysics*, **43**:167-74.

Pieraccini, M., Mecatti, D., Luzi, G., Seracini, M., Pinelli, G. & Atzeni, C., 2005. Non-contact intrawall penetrating radar for heritage survey: the search of the 'Battle of Anghiari' by Leonardo da Vinci, *NDT & E International*, **38**, 151–157.

Ríos Yanes M., 2018 2018. "Apuntes históricos sobre la iglesia mayor de Puebla", Cap. III, pp. 201-241. "*La antigua Catedral de Puebla*". Secretaria de Cultura y Turismo del Edo. De Puebla.

Rocha Martinez, R. 2011. "La vara". Boletín de Monumentos Históricos, No.28:64-79, México-INAH.

Solla, M., Lorenzo, H., Rial, F.I. & Novo, A., 2011. GPR evaluation of the Roman masonry archb ridge of Lugo(Spain), *NDT & E International*, **44**, 8–12.

Tsokas, G.N., Tsourlosi, P. I., Vargermezisis, G., and Novack, M., 2008. Non-destructive Electrical ResistivityTomography for Indoor Investigation:theCaseof KapnikareaChurch in Athens. *Archaeological Prospection,* **15**, 47-61.

Yalciner, C., Ç., Bano, M., Kadioglu, M., Karabacak, V., Meghraoui, M. and Altunel, E., 2009. New temple discovery at the Archaeological Site of Nysa (Western Turkey) using GPR method, *Journal of Archaeological Science*, Vol 36, p. 1680–1689.

Yalçıner C., Ç., 2019. Coordinated application of structural strengthening injections with GPR method for restoration of historical artifacts: example study of Bodrum castle. *Journal of Geophysics and Engineering*, Volume **16**, Issue 2, April 2019, Pages 325–331, https://doi.org/10.1093/jge/gxz009.